PROSTHETICS

2016 © The Authors, some rights reserved; exclusive licensee American Association for the Advancement of Science.

Hybrid EEG/EOG-based brain/neural hand exoskeleton restores fully independent daily living activities after quadriplegia

S. R. Soekadar,[1,2]* M. Witkowski,[1,2] C. Gómez,[3] E. Opisso,[3] J. Medina,[3] M. Cortese,[4] M. Cempini,[4] M. C. Carrozza,[4] L. G. Cohen,[5] N. Birbaumer,[2,6] N. Vitiello[4,7]

Direct brain control of advanced robotic systems promises substantial improvements in health care, for example, to restore intuitive control of hand movements required for activities of daily living in quadriplegics, like holding a cup and drinking, eating with cutlery, or manipulating different objects. However, such integrated, brain- or neural-controlled robotic systems have yet to enter broader clinical use or daily life environments. We demonstrate full restoration of independent daily living activities, such as eating and drinking, in an everyday life scenario across six paraplegic individuals (five males, 30 ± 14 years) who used a noninvasive, hybrid brain/neural hand exoskeleton (B/NHE) to open and close their paralyzed hand. The results broadly suggest that brain/neural-assistive technology can restore autonomy and independence in quadriplegic individuals' everyday life.

Downloaded from https://www.science.org at The Hong Kong University of Science and Technology (Guangzhou) on May 26, 2026

INTRODUCTION

Quadriplegia, the loss of motor function of both arms and legs, is often caused by traumatic cervical spinal cord injury (SCI) affecting 1 in 10,000 people worldwide (*1*, *2*). Although SCI is associated with lower life expectancy and quality of life (*3*, *4*), it typically affects younger individuals, leading to substantial loss of their independence and autonomy. Regaining hand and arm function was identified as the most critical need in this population (*5*). Although SCI remains an incurable condition with most treatment approaches aimed at minimizing secondary medical complications and maximizing residual function, the development of brain-machine interfaces (BMIs) has recently fueled hope that by bypassing the lesioned spinal system, independence and autonomy of individuals with severe paralysis could be restored (*6*–*9*). In particular, the possibility that repeated use of such BMI-based bypass could trigger neurological recovery despite clinically complete and chronic SCI (*10*) points to new avenues in the treatment of severe paralysis that build on fostering neuroplasticity through direct brain- or neural-robot interactions. BMIs translate electric, magnetic, or metabolic brain activity (e.g., associated with the intention to reach and grasp) into control signals of external machines, exoskeletons, or robots (*11*). Because mental imagery (e.g., the visualization of a closing hand) results in an actual hand-closing motion performed by a robotic device or exoskeleton in such a paradigm, BMI control is particularly intuitive.

Although implantable BMIs have recently been shown to allow versatile control of a robotic arm in patients with chronic quadriplegia (*8*, *12*, *13*), the required craniotomy entails the risk of surgical complications, for example, infections or bleedings. Also, implantable systems have to be explanted after some time, posing an ethical and clinical dilemma. Thus, implantation of a BMI for controlling such versatile robots is mainly attractive for individuals who are completely paralyzed, for example, after severe brainstem stroke or in the late stage of a neurodegenerative disease.

To date, we know of no patient who has used a BMI outside the laboratory to perform activities of daily living (ADLs), for example, having a full meal in an outside restaurant. The main obstacle for such application relates to the nonstationarity of brain activity and susceptibility to environmental artifacts, particularly in noninvasive brain activity recordings that provide lower signal-to-noise ratios compared with invasive recordings (*14*). Thus, hybrid systems that combine BMI technology with other biosignals (*15*–*17*) or eye gaze (*18*, *19*) to improve system control have been proposed. Previous work demonstrated that the combination of electroencephalography (EEG) and electrooculography (EOG) can be used for hand exoskeleton control in healthy volunteers under laboratory conditions (*16*, *17*). The translational value of this approach for restoration of hand function in real-life environments after quadriplegia, a condition for which there is currently no effective treatment, was not known. Here, we address this question and show the restoration of fully independent ADLs, such as eating and drinking, across six quadriplegic individuals with cervical SCI.

Study participants used a noninvasive brain/neural hand exoskeleton (B/NHE) that translates brain electric signals accompanying the intention to grasp into actual exoskeleton-driven hand-closing motions and EOG signals related to voluntary horizontal eye movements [horizontal oculoversions (HOVs)] into exoskeleton-driven hand-opening motions (Figs. 1 and 2). The participants were asked to perform self-initiated reaching and grasping actions, for example, eating and drinking in a nearby restaurant and outdoors. The ability to grasp and manipulate daily life objects was assessed using the Toronto Rehabilitation Institute–Hand Function Test (TRI-HFT) with and without the B/NHE system. Reliability, tolerability, and practicability to perform ADLs were rated by each participant after the end of the session.

RESULTS

Functioning in ADLs and hand motor function before B/NHE control

Evaluation of functioning in ADLs using the Spinal Cord Independence Measure (SCIM) and Functional Independence Measure (FIM)

[1]Applied Neurotechnology Laboratory, Department of Psychiatry and Psychotherapy, University Hospital Tübingen, Tübingen, Germany. [2]Institute of Medical Psychology and Behavioral Neurobiology, University of Tübingen, Tübingen, Germany. [3]Hospital de Neurorehabilitació Institut Guttmann, Barcelona, Spain. [4]BioRobotics Institute, Scuola Superiore Sant'Anna, Pisa, Italy. [5]Human Cortical Physiology and Stroke Neurorehabilitation Section, National Institutes of Neurological Disorders and Stroke, National Institutes of Health, Bethesda, MD 20892, USA. [6]Ospedale San Camillo, IRCCS, Venice, Italy. [7]Fondazione Don Carlo Gnocchi, Firenze, Italy.
*Corresponding author. Email: surjo.soekadar@uni-tuebingen.de

underlined that all participants were severely compromised in their independence [SCIM score, 40.0 ± 17.6 (maximum score is 100, with 0 denoting complete dependence and 100 indicating complete independence)] and suffered from severe motor dysfunction, leading to dependence on others [FIM motor subscale score, 39.17 ± 21.62 (maximum score is 91, with 13 denoting complete dependence and 91 indicating complete independence)]. Analysis of TRI-HFT scores [total average = mean sum score of subtests 1 to 19 ± SD (maximum sum score is 133); average part 1 = mean sum score of subtests 1 to 10 ± SD (maximum sum score is 70); average part 2 = mean sum score of subtests 11 to 19 ± SD (maximum sum score is 63); mean score across subtests = average score of subtests 1 to 19 ± SD (maximum score is 7)] assessed before B/NHE application evidenced substantial deficits in grasping and manipulating the test items (total average = 72.33 ± 26.17; median = 81.00 ± 26.12; average part 1 = 37.7 ± 12.83; average part 2 = 34.83 ± 15.9; mean score across subtests = 3.81 ± 1.38).

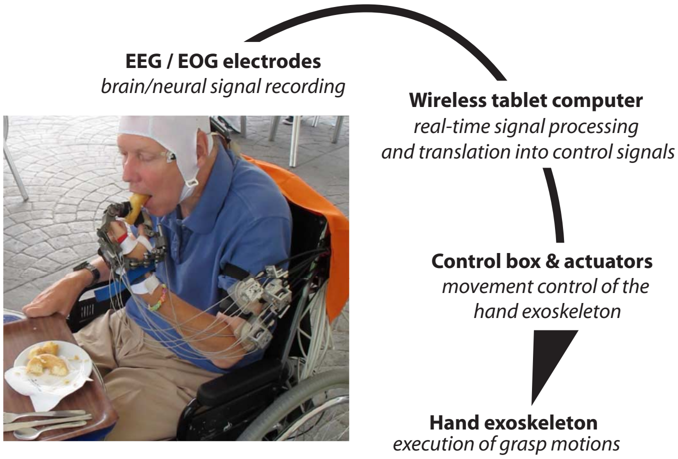

Fig. 1. Scheme of process pipeline to control the hand exoskeleton. EEG and EOG signals were transmitted to a wireless tablet computer performing real-time signal processing and translation into control signals sent to a control box and actuators moving the hand exoskeleton via a flexible cable sheath system.

Providing a portable B/NHE system for application in daily life

Integration of portable, battery-driven, and partly wireless brain/neural-computer interaction (BNCI) components into a standard wheelchair enabled the study participants to move freely with the B/NHE outside the laboratory and outdoors. Activation and deactivation of the B/NHE system could be performed over a portable and wireless tablet computer stored under the seat (Fig. 3, B and C). After calibration and familiarization with the system over 8 to 10 min, all participants were able to control hand-opening and interruption of unintended hand exoskeleton motions using HOV as measured by EOG (fig. S1). Participants used the system for up to 4 hours without the need to recharge any of the components. By translating EEG sensorimotor rhythm (also termed μ-rhythm; 8 to 13 Hz) event-related desynchronization (SMR-ERD) (fig. S2), reaching a threshold value (Fig. 2B) specific to the intention

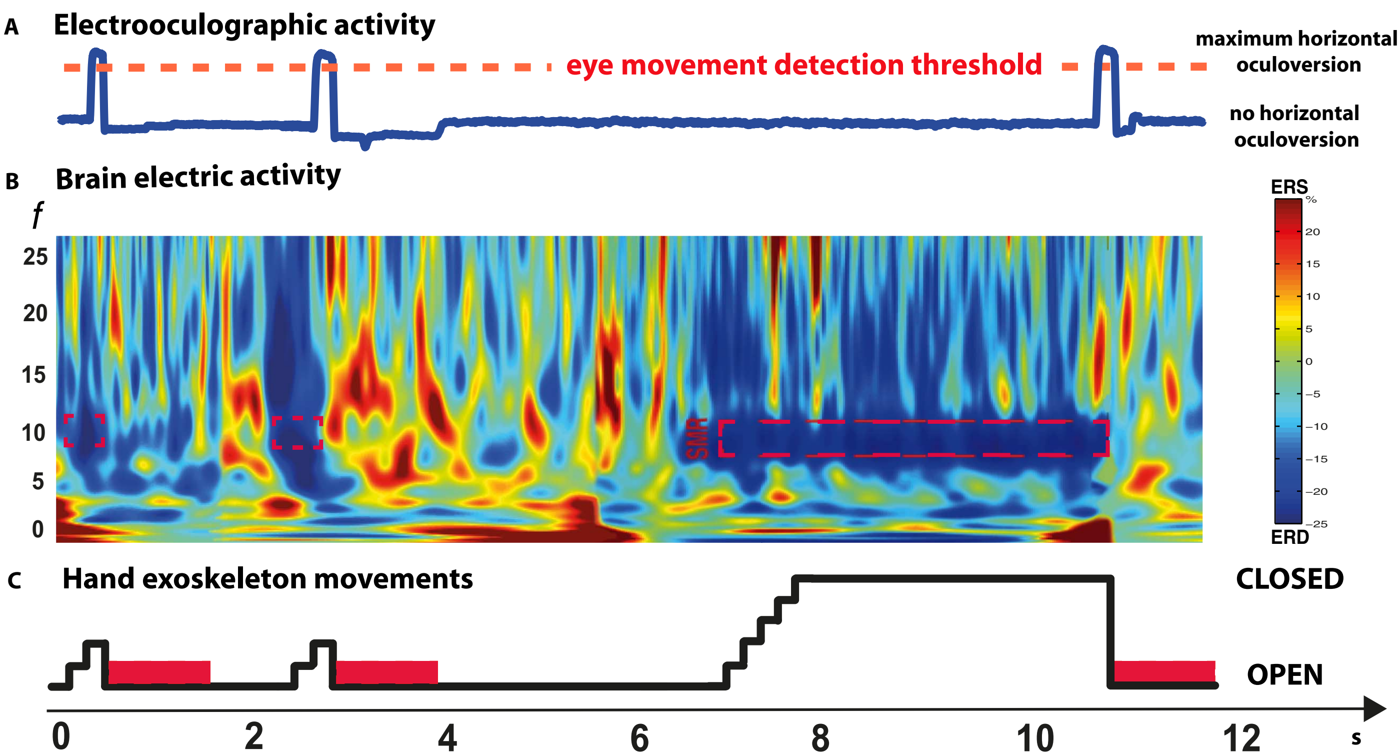

Fig. 2. Design of hybrid biosignal processing for reliable hand exoskeleton control. Signals related to the detection of HOVs and intention to grasp as measured by electrooculographic (**A**) and brain electric (**B**) activity were used for the hybrid BMI hand exoskeleton control (**C**). Hand exoskeleton closing movements were initiated by the detection of SMR-ERD, whereas hand exoskeleton opening movements were controlled by HOVs' EOG activity exceeding the eye movement detection threshold [red dashed line in (A)]. In case EOG activity exceeded the eye movement detection threshold during SMR-ERD [indicated by the red dashed rectangle in (B)], the hand exoskeleton opened, and brain control was blocked for 1.5 s [indicated by the red rectangles in (C)] to ensure safety during performing daily life actions.

Downloaded from https://www.science.org at The Hong Kong University of Science and Technology (Guangzhou) on May 26, 2026

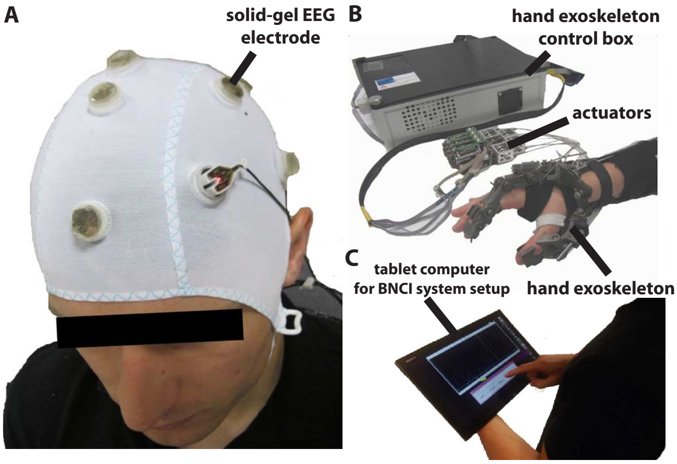

Fig. 3. Illustration of the different components of the B/NHE system. (**A**) An elastic and air-permeable cap with holders for solid-gel electrodes to record EEG was attached to the participant's head. (**B**) Control unit with battery, actuators, and lightweight hand exoskeleton to perform grasping motions. The control box and actuators were incorporated into a standard wheelchair, allowing the participants to use the system outside the laboratory. (**C**) Brain signals related to grasp movement intentions were transmitted to a wireless tablet computer, which analyzes and translates them into control signals of a hand exoskeleton.

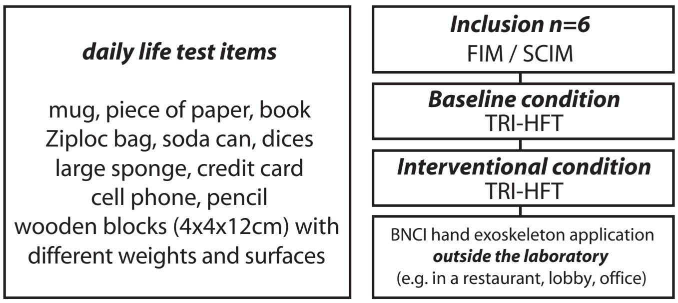

Fig. 4. List of daily life objects used for hand function assessment as measured by the TRI-HFT (left) and study design (right).

to perform right hand grasping motions, into closing motions of the lightweight robotic hand exoskeleton (*20*, *21*), participants grasped, securely held, and manipulated objects requiring hand gripping spans of up to 10 cm (Fig. 4). Because detection of the intention to grasp was specific to SMR-ERD at electrode C3 located in proximity to the hand knob area of the primary motor cortex, participants could speak or move the shoulder without initializing B/NHE movements (see movie S5).

Hand motor function during B/NHE control

Under B/NHE control, TRI-HFT scores increased significantly (total average = 113.33 ± 10.21; median = 113.25 ± 10.21; average part 1 = 50.33 ± 10.25; average part 2 = 63.00 ± 0.00; mean score across subtests = 5.96 ± 0.54) ($Z = -2.1024$, $r = -0.8583$, $P < 0.05$) (Fig. 5) (Tables 1 and 2 and Supplementary Analysis). Hand function across participants reached 84.96 ± 7.19% of the maximum score, translating into full restoration of independent ADLs requiring lateral pinch grasp and object manipulation such as independent eating and drinking. Interrater reliability was high. Average intraclass correlation coefficient (ICC) was 0.96 with a 95% confidence interval from 0.95 to 0.97 [$F(227, 227) = 25$; $P < 0.01$].

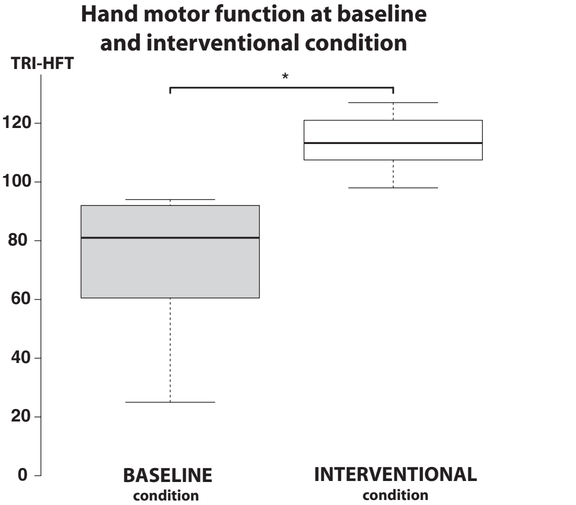

Fig. 5. Difference in hand motor function as measured by the TRI-HFT before (baseline condition) and during application of the B/NHE system (interventional condition) across all participants. Hand motor function reached almost normal levels during the interventional condition (84.96 ± 7.19% of the maximum score) independent of the severity of the paralysis. Centerlines show the medians. Box limits indicate the 25th and 75th percentiles. *$P < 0.05$.

B/NHE control in daily life environments

Participants could control the B/NHE outside the laboratory, for example, in a restaurant or outdoors at their own choice, and performed different tasks, including grasping a bottle and drinking (movies S1 and S2), grasping a fork and eating (movie S3), grasping and handing over a credit card (movie S4), eating potato chips with bare fingers (movie S5), or signing a document with a pen (movie S6), which they could not do without the B/NHE. During use of the system, 16.3 ± 4.5% of exoskeleton-driven closing motions were interrupted by EOG documenting successful control and safety of the system (fig. S3). Participants reported that the B/NHE was reliable and practical when performing ADLs ($P < 0.01$). No side effects or any discomforts related to the B/NHE system were reported (fig. S4).

DISCUSSION

Data presented here show full restoration of independent ADLs, such as having a full meal or signing a document with a pen, using a hybrid B/NHE system in an everyday life environment across six patients with chronic quadriplegia who were previously unable to perform these tasks unassisted. Whereas the B/NHE performed grasping motions upon intended finger movements of the paralyzed hand and fingers, interruption of unintended grasping motions and reset of the B/NHE system into an open position was controlled by HOVs. Using the system, paralyzed individuals who are unable to grasp and manipulate any large and heavy object, like a full can or cup, could securely grasp, lift, hold, and manipulate such objects at their own volition. Application of the system did not require any extensive learning protocol and could be used after a short calibration period of a few minutes. Also, system mounting and unmounting required only a few minutes. Use of solid-gel electrodes made hair washing after the session unnecessary; a substantial disadvantage when using conventional wet electrodes is that electrolytes and salts are left in the (paralyzed) user's hair. Besides demonstrating feasibility, tolerability, and usefulness in restoring hand function in a real-life environment

Downloaded from https://www.science.org at The Hong Kong University of Science and Technology (Guangzhou) on May 26, 2026

Table 1. TRI-HFT part 1. Grasp, lift, and object manipulation. Values are shown as means ± SD. 0, no movement elicited, that is, participant was unable to reach the object; 1, participant was able to reach the object but unable to grasp the object; 2, participant was able to reach and grasp using passive grasp but unable to lift the object successfully off the supporting surface; 3, participant was able to reach and grasp using active grasp but unable to lift the object successfully off the supporting surface; 4, participant was able to reach, grasp, and lift the object completely off the supporting surface using passive grasp but unable to manipulate the object; 5, participant was able to reach, grasp, and lift the object completely off the supporting surface using active grasp but unable to manipulate the object; 6, participant was able to reach, grasp, and lift the object completely off the supporting surface and manipulate the object using passive grasp appropriately; 7, participant was able to reach, grasp, and lift the object completely off the supporting surface and manipulate the object using active grasp appropriately/normal function.

Object	TRI-HFT score (0–7) without the B/NHE system	TRI-HFT score (0–7) with the B/NHE system
Mug (filled, 350–400 g)	5.67 ± 2.33	6.67 ± 0.82
Book (200 pages, 250 g)	4.42 ± 2.62	5.92 ± 1.86
Pop can (full, 355 ml)	2.25 ± 1.80	4.00 ± 3.29
Sponge (40 cm × 20 cm × 10 cm)	2.83 ± 2.31	6.25 ± 1.84
Mobile phone (80–100 g)	4.33 ± 2.79	4.75 ± 2.68
Paper (8 ½ inches × 11 inches, A4)	2.33 ± 2.55	5.92 ± 2.43
Ziploc bag (filled with five golf balls)	5.08 ± 2.49	6.92 ± 0.20
Dice (standard)	6.33 ± 1.20	6.92 ± 0.20
Credit card (standard)	0.92 ± 0.20	1.00 ± 0.00
Pencil (hexagonal, 0.6 cm × 19 cm)	3.33 ± 2.78	2.00 ± 2.45
Total score	**37.7 ± 12.83**	**50.33 ± 10.25**

Table 2. TRI-HFT part 2. Strength/stability of grip. Values are shown as means ± SD. Wooden blocks had the following dimensions: 40 mm × 40 mm × 120 mm. Low friction, overhead transparency sheet; polished wood, polished wood surface; high friction, Dycem nonslip material. See Table 1 for more details.

Object, rectangular block	TRI-HFT score (0–7) without the B/NHE system	TRI-HFT score (0–7) with the B/NHE system
100 g, high friction	5.00 ± 2.93	7.00 ± 0
100 g, polished wood	4.67 ± 2.80	7.00 ± 0
100 g, low friction	4.17 ± 2.67	7.00 ± 0
200 g, high friction	4.75 ± 2.86	7.00 ± 0
200 g, polished wood	2.50 ± 1.69	7.00 ± 0
200 g, low friction	3.42 ± 2.00	7.00 ± 0
300 g, high friction	4.92 ± 2.50	7.00 ± 0
300 g, polished wood	3.12 ± 2.63	7.00 ± 0
300 g, low friction	2.25 ± 1.42	7.00 ± 0
Total score	**34.83 ± 15.9**	**63.00 ± 0.00**

after quadriplegia, the reported findings provide the necessary data to design and power confirmatory multicenter-controlled clinical trials.

Although use of brain activity to control assistive devices is particularly appealing because of its direct relation to movement planning and execution, nonstationarity and susceptibility of noninvasive recordings to artifacts limit daily life applicability. However, when combined with other biosignals (e.g., EOG, as shown here), these disadvantages can be compensated for, providing system control that does not require any extensive learning procedure and that is safe for use in daily life. It is possible, though, that implementation of more powerful signal processing and statistical tools could lead to an approach with similar or better results in terms of system control using brain activity or gaze control only. Also, individual identification of scalp positions providing the optimal EEG site to detect modulations of brain activity associated with intended finger movements might further improve reliability and practicability of B/NHE control (e.g., by requiring fewer electrodes).

Although implantable recording and stimulating electrodes could achieve more versatile decoding and execution of hand movements, risks associated with implantation of such electrodes limit broader acceptance and application of this technology. Thus, detection of movement intention as demonstrated here using noninvasive EEG electrodes may remain a viable and practical means of incorporating brain/neural signals into the control of real-time assistive technology applicable outside a laboratory environment that will be broadly accepted in the near future. Use of EOG or other peripheral biosignals alone would not provide the high level of intuitiveness associated with direct translation of brain activity into actual movements delivered by a hand exoskeleton. Other noninvasive assistive systems that use surface functional electric stimulation or other neuroprosthetic approaches in SCI could not restore hand function to a level comparable to that demonstrated here (*22–24*).

However, there are some limitations related to the use of hand exoskeletons for motor restoration, for example, the added weight put on the user's hand and arm, possible restrictions in the hand's degrees of freedom (DOFs) depending on the number of the exoskeleton's artificial joints, metal component fatigue, and natural wear of the working parts. Individuals without sufficient shoulder and arm motor function may not benefit from such approach because of their inability to reach out with the hand exoskeleton. The methodology's overall clinical validity to restore ADLs after quadriplegia has to be tested in larger clinical trials. The required time to perform a specific grasping task depends on the preset speed of hand exoskeleton–driven finger motions. In case of remaining hand and finger function, it is thus possible that users require more time to perform the same function with the B/NHE than without the system. Also, mounting and unmounting the hand exoskeleton system used in this study required third-person assistance. The ability to pick up and manipulate very small objects (e.g., a pencil, <1 cm^3) did not improve due to the buildup of the exoskeleton's fingertips. The TRI-HFT required participants to pick up a pencil lying flat on a table, and some participants who were able to use passive grasp to perform such task without the B/NHE scored lower with the B/NHE attached. However, moving the pen to the desk's border enabled the participants to grasp, lift, and even write with the pen using the B/NHE (see movies S1 to S7). Also, the tested robotic system did not adjust grip force according to the characteristics of the grasped objects, such as weight

Downloaded from https://www.science.org at The Hong Kong University of Science and Technology (Guangzhou) on May 26, 2026

or fragility. More intelligent systems that provide sensory feedback to the user and adapt exerted forces according to the objects that are manipulated may further improve the practicability of the system. Inclusion of context awareness (e.g., using three-dimensional object recognition, inertial motion capturing, or other sensor technologies) may further improve real-life applicability of B/NHE systems by reducing false-positive classifications related to, for example, head turning during object manipulation, unforeseen user behavior, or unanticipated situations. It is conceivable that all named technical problems can be solved in the near future. Given the high level of function the participants regained with the system, several ethical considerations will have to be addressed as well, for example, availability, supply, and assumption of costs of such assistive technology. Before entering the study, participants of this clinical trial were informed and agreed that B/NHE would not be available after their participation and would be removed at the end of the session.

Recently, clinical studies indicated that repeated use of BMI-driven exoskeletons could trigger lower limb motor recovery after complete SCI (*10*) and facilitate upper limb motor recovery after chronic stroke when coupled with behavioral physical therapy (*25*). In these studies, severely paralyzed patients received contingent proprioceptive, haptic, and visual feedback related to brain activity associated with the intention to move their paralyzed limbs (*10*, *25*–*28*). Clinical improvements were accompanied by functional and structural reorganization of the central nervous system quantified by functional magnetic resonance imaging (*25*), diffusion tensor imaging (*26*, *28*), and EEG recordings (*10*).

Although these studies were conducted at clinical centers and required a considerable amount of resources, a B/NHE as introduced and tested here could be used as an effective tool to foster upper limb motor recovery in everyday life environments. In particular, the possibility to apply such technology in the user's normal environment and on a daily basis may substantially facilitate generalization of learned motor skills (*9*) and may prove to be more effective than previous BMI protocols.

Besides having a substantial impact on improving the autonomy and independence of individuals with severe motor disabilities, such as paralysis after cervical SCI as exemplified here, merging direct brain/neural control with advanced robotic systems may also lead to substantial improvements in other areas of health care, for example, substituting or restoring sensory or cognitive deficits.

MATERIALS AND METHODS

Participants

Six BNCI-naïve individuals (five male; mean age, 30 ± 14 years; P1 to P6) with complete [n = 3; American Spinal Injury Association (ASIA) grades A and B] and incomplete (n = 3; ASIA grades A, B, and C) cervical SCI (C4 to C6) were invited to the Institut Guttmann Hospital de Neurorehabilitación (Badalona, Spain) to participate in a one-arm, open-trial, repeated-measures study (Clinical Trials Identifier, NCT02336321).

Participants were selected on the basis of the following inclusion criteria: ASIA impairment scale grades A, B, and C (lower extremity motor score, <20); motor level of injury from cervical level four to seven (C4 to C7) according to ASIA guidelines; nonpregnant, nonlactating female; age between 15 and 65 years; and time since SCI at least 12 months. Possible candidates were excluded if they met one of the following criteria: history of severe neurological injuries other than SCI (e.g., multiple sclerosis, cerebral palsy, amyotrophic lateral sclerosis, traumatic brain injury, or stroke), concurrent other medical diseases (e.g., infections, circulatory, heart, or lung disorders) interfering with the study, unstable spine or unhealed limbs or pelvic fractures, severe spasticity (Ashworth grade of ≥4) or uncontrolled clonus, diagnosis of severe osteoporosis/osteopenia, psychiatric or cognitive conditions that may interfere with the trial, and inability to provide informed consent.

Before application of the B/NHE, all participants underwent thorough clinical examination, including assessments of the SCIM and FIM motor subscale. Whereas the SCIM evaluates the overall independency and ability to perform conventional ADLs across three domains [(i) self-care: six items, scores range from 0 to 20; (ii) respiration and sphincter management: four items, scores range from 0 to 40; (iii) mobility: nine items, scores range from 0 to 40; total SCIM score ranges from 0 to 100, with 0 denoting complete dependence, <60 indicating severely compromised in independence, <80 denoting moderately compromised in independence, and 100 indicating complete independence], including indoor and outdoor ambulation, the FIM motor subscale reflects the burden of care to effectively perform basic movement-related ADLs, such as eating, grooming, or dressing [13 subtests; subscore range, 1 to 7, with 1 denoting total assistance required and 7 indicating no assistance required; minimum sum score is 13 (complete dependence); maximum sum score is 91 (complete independence)].

Before inclusion, participants gave their written informed consent, including photography and video, and agreed that this material can be used in journals and other public media. The study protocol was approved by the local ethics committee of the Institut Guttmann Hospital de Neurorehabilitación (Badalona, Spain).

BNCI system

All participants sat in a wheelchair while EEG was recorded from five conventional EEG recording sites (F3, T3, C3, P3, and CZ, according to the international 10/20 system) using polyamide-based solid-gel electrodes with a diameter of 1 cm (*29*). EEG signals were amplified using an actiCAP system linked to a BrainAmp (Brain Products, Gilching, Germany) unit. A reference electrode was placed at FCz and a ground electrode was placed at Fz. EEG was recorded with a sampling rate of 200 Hz and band-pass–filtered at 0.4 to 70 Hz. On the basis of previous studies, a surface Laplacian filter was used, showing superior performance in detecting focal SMR-ERD while attenuating activity from distant sources (such as electromyographic activity, eye movements, blinks, or other alpha rhythm sources) compared with other approaches (*30*). Moreover, surface Laplacian filtering showed to be particularly suitable for BMI applications because no volume conductor model or detailed specification of neural sources was required, resulting in low computational costs (*31*).

EOG was recorded from the standard EOG recording site at the right outer canthus. Biosignals were translated into control signals of the exoskeleton using the BCI2000 software platform (*32*). During calibration, the reference value (RV) of SMR-ERD related to externally paced intended grasping movements of the right hand was calculated by using a power spectrum estimation based on an autoregressive model of order 16 (Burg algorithm) (*16*, *17*, *27*). Calculation of the RV comprised a total of 42 trials, each lasting 5 s, followed by an intertrial interval of 4 s, during which participants were inactive. The optimal frequency for SMR-ERD detection [frequency of interest (FOI)] was set to the frequency showing the highest SMR-ERD modulation during intended movements in the range 8 to 13 Hz (table S1). For online classification of SMR-ERD, a frequency filter with an FOI of ±1.5 Hz was used. A detection threshold for movement initiation and execution was calculated on the basis of the additional 42 trials, during

Downloaded from https://www.science.org at The Hong Kong University of Science and Technology (Guangzhou) on May 26, 2026

which participants received online visual feedback of SMR-ERD. The detection threshold was set at two SDs above average SMR-ERD and used for online B/NHE control. The brain electric activity had to exceed the SMR-ERD detection threshold for at least 1.5 s to achieve a complete closing motion. The source code and software used for this study are available as Supplementary Materials (see Supplementary Source Codes and Software). As a next step, participants were instructed to perform 20 externally paced maximum eye movements to the left or to the right (HOVs) starting from a fixation cross in front of them following a visual cue while EOG was recorded. Such maximum eye movements usually do not occur during everyday life routines and circumstances, so their specificity to signify an intentional event is very high. An HOV detection threshold was set at two SDs below the average EOG signal recorded during maximum HOV. If EOG signals exceeded this threshold, the hand exoskeleton was stopped and moved to an open position, whereas closing movements were blocked for 1.5 s (Fig. 2, A and C, and fig. S1). Calibration of the system required about 9 min. Participants reported after the session that the calibration process was easy to follow (fig. S4). To assess and verify reliable translation of EEG and EOG signals into exoskeleton-driven hand opening and closing motions, mean SMR-ERD values as well as false-positive rates (FPRs), defined as the number of exoskeleton-driven hand closing motions that were interrupted by HOV, were calculated for each participant (figs. S2 and S3).

Hand exoskeleton

A battery-driven electromechanical orthosis for active assistance of the thumb and index fingers was used. The system consisted of a wearable and lightweight articulated part fixed to the fingers and hand dorsum of the user (*20*, *21*), as well as a remote actuation block with multiple motors and a power supply/battery unit. By embedding features such as cable-driven underactuation, increased adaptability, and compliance with individual hand shapes based on passive DOF, as well as self-alignment mechanisms to compensate for joint axes misplacements, the design of the hand exoskeleton used in this study strived for maximizing functional DOF (fDOF) and human kinematic compatibility, wearability, and portability (*21*).

Components of the wearable part consisted of titanium alloy and were arranged into an ergonomic multiphalanx apparatus that provided passive and active DOF, allowing for both finger motion actuation and alignment to the individual user anthropometry. Four DOFs were independently activated in the system: two for the index finger flexion, one for the thumb flexion, and one for the thumb opposition. The total weight of the system attached to the hand was 438 g. Commanded motion was transmitted from the actuation block through a flexible cable sheath system, and all active DOFs were bidirectionally actuated. On the basis of previous evaluations of postural hand synergies (*33*) and relevance of different grasp types in ADLs (*34*), movement trajectories for each participant were set to result in palmar grasp for objects larger than 3 cm (e.g., a soda can, a sponge, or a cell phone) and lateral pinch for objects measuring less than 3 cm. The actuation block embedded seven brushed direct current (DC) electric motor gears (four of which were used in the study) that provided an independent motion source and applied a maximum force of 5 N. Two position closed-loop controls were used for the motor axes and DC motors through custom current servo amplifiers. Real-time control was provided using NI single-board RIO running a real-time operating system (National Instruments, Austin, TX). Mechanical coupling between the actuator and the exoskeleton effector was provided by means of latchable mating capstan pulleys guided along the user's right upper limb. This ensured minimum restraint of hand and arm motions owing to the parts fixed to the upper limb because the control box and battery unit (providing energy supply for up to 6 hours) were stored under the seat of the wheelchair, allowing quadriplegic individuals to use the B/NHE outside the laboratory.

Primary outcome measure, videotaping, and safety

To quantify differences in hand motor function before and during application of the B/NHE, the TRI-HFT (a measure to assess the capability to grasp and manipulate various daily life objects with different weights, shapes, surfaces, and textures) was performed without the B/NHE (baseline condition) and while participants were wearing the B/NHE (interventional condition). The TRI-HFT was performed about 30 min before and after the B/NHE was attached to the participant's body and consisted of two parts with a total of 19 subtests (part 1, 10 subtests; part 2, 9 subtests) that are equally weighted. The first part includes manipulation of different objects, whereas the second part measures the strength and stability of palmar grasp. Tests were administered and guided sequentially by an occupational therapist or physician. Before each trial, the administrator demonstrated the correct performance of the task the individual should perform. Time to perform any of the trials was not restricted, and participants could indicate the end of the trial if they decided that accomplishing the task at a higher score was not possible. A video camera was positioned opposite to the participant at a 45° angle at a height of about 1 m. All trials were videotaped, and videos were stored for further processing and evaluation. In part 1, the following 10 items were used: a mug, a book, a soda can, an isosceles triangular sponge, a wireless home telephone, a paper sheet, a Ziploc bag filled with five golf balls, a dice, a credit card, and a pencil. Grasping and manipulation of these objects were rated on a scale ranging from 0 ("no movement possible") to 7 ("participant was able to reach, grasp, and lift the object completely off the supporting surface and manipulate the object using active grasp appropriately/normal function") (for more details on the rating scale, see Table 2). A mean score of less than 4 across subtests (corresponding to a TRI-HFT total average score of ≤76) indicates the inability to manipulate most tested items; a mean score of 6 and above (corresponding to a TRI-HFT total average score of ≥114) indicates successful object manipulation across subtests.

During the second part of the test, the following items were used: nine rectangular wooden blocks, an instrumented cylinder, a credit card attached to a dynamometer, and a wooden bar. Whereas grasping, lifting, and manipulating the wooden blocks reflect the ability and strength of palmar grasps (also rated on a scale from 0 to 7), the latter three items measure the torque and force the grasp could resist and the eccentric load the participant could sustain with and without the hand exoskeleton. Because this latter component of the second part is rated in Newton and does not reflect the capability of manipulating daily life objects but rather the forces here exerted by the motorized hand exoskeleton, this part was not included as a primary outcome measure. The maximum score of the TRI-HFT was thus 133 points (part 1, 70; part 2, 63).

During the test, objects were placed on a desk at a distance of 20 to 30 cm from the participant. The participants were expected to pick up the object, lift it completely off the supporting surface, hold it, manipulate it, and place it back on the table. Participants could interrupt the trials whenever needed, and B/NHE control could be overridden and stopped by both the experimenter and the participants in case of any safety risk using a red emergency button (Fig. 2B). The capability to grasp and manipulate each TRI-HFT item was rated by two independent

Downloaded from https://www.science.org at The Hong Kong University of Science and Technology (Guangzhou) on May 26, 2026

experts (a physical therapist and a physician). The TRI-HFT score for each individual was calculated as the average of all raters (for distribution of scores in each subtest, see fig. S5). An SD across participants was calculated for each subtest and each part of the test. Because the TRI-HFT is the only validated clinical assessment tool that includes manipulation of daily life objects and specifically tests for dexterity and strength after SCI, the TRI-HFT was regarded particularly suitable for this study. Providing excellent reliability ($r = 0.98$), the TRI-HFT accounts for the individual's ability in completing the different stages of grasping tasks (i.e., reach and grasp, lift, and manipulate), resulting in high sensitivity to change in function (*35*).

Application of the B/NHE outside the laboratory and outdoors

After mounting the B/NHE, participants were asked to move outside the laboratory, for example, to a restaurant, a lobby, an outdoor terrace, or an office environment. In these different environments, participants could perform various tasks that included grasping a bottle and drinking, grasping a fork and eating, grasping and handing over a credit card, eating potato chips with bare fingers, or signing a document with a pen. Overall, the whole experimental session took about 3.5 hours per participant.

At the end of the session, participants were asked whether they felt that using the system was reliable and practical when performing ADLs and to report any side effects or discomforts that they experienced during the experimental session (fig. S4). Thereafter, all parts of the B/NHE that were attached to the participants' head and arm were removed.

Offline data analysis and statistics

TRI-HFT scores were evaluated for each participant and averaged over the whole group. To test for a difference in the TRI-HFT scores before and during the application of the B/NHE, a Wilcoxon signed-rank test was applied using the package "coin" in R (*36*). An exact *P* value that incorporated ties using the Pratt method (*37*) was calculated. Agreement in scores between raters was tested by calculating the ICC (*38*) that reflects the proportion of variability in observations due to differences between pairs of scores using the following equation [ICC3 according to (*39*)]

$$\text{ICC} = \frac{(\text{BMS} - \text{EMS})}{\text{BMS} + (n-1)\text{EMS}}$$

where BMS is the between-subjects mean square, EMS is the error mean square, and n is the number of raters. The ICC can range from 0 (no agreement) to 1 (perfect agreement). To evaluate the participants' responses regarding the reliability and practicability to perform ADLs, a one-sample binomial test was applied.

SUPPLEMENTARY MATERIALS

robotics.sciencemag.org/cgi/content/full/1/1/eaag3296/DC1
Fig. S1. Flowchart of the B/NHE control loop.
Fig. S2. Mean SMR-ERD and SMR event-related synchronization during experimental sessions across participants.
Fig. S3. Mean FPR in the detection of intended hand-closing motions during hybrid B/NHE control across participants.
Fig. S4. Usability and user experience survey using a five-level Likert scale.
Fig. S5. Distribution of TRI-HFT scores across participants in each subtest.
Table S1. Optimal frequency for SMR-ERD detection across study participants.
Supplementary Analysis
Supplementary Source Codes and Software
Movie S1. Summary video.
Movie S2. Grasping a bottle and drinking.
Movie S3. Grasping a fork and eating.
Movie S4. Grasping and handing over a credit card.
Movie S5. Eating potato chips with "bare" fingers.
Movie S6. Signing a document with a pen.
Movie S7. Volunteer grasping cutlery at the table border and throwing a dice with the B/NHE.

REFERENCES AND NOTES

1. A. Singh, L. Tetreault, S. Kalsi-Ryan, A. Nouri, M. G. Fehlings, Global prevalence and incidence of traumatic spinal cord injury. *Clin. Epidemiol.* **6**, 309–331 (2014).
2. J. C. Furlan, B. M. Sakakibara, W. C. Miller, A.V. Krassioukov, Global incidence and prevalence of traumatic spinal cord injury. *Can. J. Neurol. Sci.* **40**, 456–464 (2013).
3. D. J. Strauss, M. J. DeVivo, D. R. Paculdo, R. M. Shavelle, Trends in life expectancy after spinal cord injury. *Arch. Phys. Med. Rehabil.* **87**, 1079–1085 (2006).
4. M. L. Campbell, D. S. Sheets, P. S. Strong, Secondary health conditions among middle-aged individuals with chronic physical disabilities: Implications for unmet needs for services. *Assist. Technol.* **11**, 105–122 (1999).
5. K. D. Anderson, Targeting recovery: Priorities of the spinal cord-injured population. *J. Neurotrauma* **21**, 1371–1383 (2004).
6. D. Borton, S. Micera, J. del R. Millán, G. Courtine, Personalized neuroprosthetics. *Sci. Transl. Med.* **5**, 210rv2 (2013).
7. T. Isa, Y. Nishimura, Plasticity for recovery after partial spinal cord injury—Hierarchical organization. *Neurosci. Res.* **78**, 3–8 (2014).
8. C. E. Bouton, A. Shaikhouni, N. V. Annetta, M. A. Bockbrader, D. A. Friedenberg, D. M. Nielson, G. Sharma, P. B. Sederberg, B. C. Glenn, W. J. Mysiw, A. G. Morgan, M. Deogaonkar, A. R. Rezai, Restoring cortical control of functional movement in a human with quadriplegia. *Nature* **533**, 247–250 (2016).
9. S. R. Soekadar, N. Birbaumer, M. W. Slutzky, L. G. Cohen, Brain–machine interfaces in neurorehabilitation of stroke. *Neurobiol. Dis.* **83**, 172–179 (2015).
10. A. R. C. Donati, S. Shokur, E. Morya, D. S. F. Campos, R. C. Moioli, C. M. Gitti, P. B. Augusto, S. Tripodi, C. G. Pires, G. A. Pereira, F. L. Brasil, S. Gallo, A. A. Lin, A. K. Takigami, M. A. Aratanha, S. Joshi, H. Bleuler, G. Cheng, A. Rudolph, M. A. L. Nicolelis, Long-term training with a brain-machine interface-based gait protocol induces partial neurological recovery in paraplegic patients. *Sci. Rep.* **6**, 30383 (2016).
11. J. R. Wolpaw, Brain–computer interfaces. *Handb. Clin. Neurol.* **110**, 67–74 (2013).
12. L. R. Hochberg, D. Bacher, B. Jarosiewicz, N. Y. Masse, J. D. Simeral, J. Vogel, S. Haddadin, J. Liu, S. S. Cash, P. van der Smagt, J. P. Donoghue, Reach and grasp by people with tetraplegia using a neurally controlled robotic arm. *Nature* **485**, 372–375 (2012).
13. J. L. Collinger, B. Wodlinger, J. E. Downey, W. Wang, E. C. Tyler-Kabara, D. J. Weber, A. J. McMorland, M. Velliste, M. L. Boninger, A. B. Schwartz, High-performance neuroprosthetic control by an individual with tetraplegia. *Lancet* **381**,557–564 (2013).
14. T. Ball, M. Kern, I. Mutschler, A. Aertsen, A. Schulze-Bonhage, Signal quality of simultaneously recorded invasive and non-invasive EEG. *Neuroimage* **46**, 708–716 (2009).
15. G. R. Müller-Putz, C. Breitwieser, F. Cincotti, R. Leeb, M. Schreuder, F. Leotta, M. Tavella, L. Bianchi, A. Kreilinger, A. Ramsay, M. Rohm, M. Sagebaum, L. Tonin, C. Neuper, J. R. Del Millán, Tools for brain-computer interaction: A general concept for a hybrid BCI. *Front. Neuroinform.* **5**, 30 (2011).
16. S. R. Soekadar, M. Witkowski, N. Vitiello, N. Birbaumer, An EEG/EOG-based hybrid brain-neural computer interaction (BNCI) system to control an exoskeleton for the paralyzed hand. *Biomed. Tech.* **60**, 199–205 (2015).
17. M. Witkowski, M. Cortese, M. Cempini, J. Mellinger, N. Vitiello, S. R. Soekadar, Enhancing brain-machine interface (BMI) control of a hand exoskeleton using electrooculography (EOG). *J. Neuroeng. Rehabil.* **11**, 165 (2014).
18. E. C. Lee, J. C. Woo, J. H. Kim, M. Whang, K. R. Park, A brain–computer interface method combined with eye tracking for 3D interaction. *J. Neurosci. Methods* **190**, 289–298 (2010).
19. T. O. Zander, M. Gaertner, C. Kothe, R. Vilimek, Combining eye gaze input with a brain–computer interface for touchless human–computer interaction. *Int. J. Hum.-Comput. Int.* **27**, 38–51 (2010).
20. M. Cortese, M. Cempini, P. R. de Almeida Ribeiro, S. R. Soekadar, M. C. Carrozza, N. Vitiello, A mechatronic system for robot-mediated hand telerehabilitation. *IEEE/ASME Trans. Mechatron.* **20**, 1753–1764 (2015).
21. M. Cempini, M. Cortese, N. Vitiello, A powered finger-thumb wearable hand exoskeleton with self-aligning joint axes. *IEEE/ASME Trans. Mechatron.* **20**, 705–716 (2015).
22. G. J. Snoek, M. J. Ijzerman, F. A. in 't Groen, T. S. Stoffers, G. Zilvold, Use of the NESS handmaster to restore handfunction in tetraplegia: Clinical experiences in ten patients. *Spinal Cord* **38**, 244–249 (2000).
23. G. Alon, K. McBride, Persons with C5 or C6 tetraplegia achieve selected functional gains using a neuroprosthesis. *Arch. Phys. Med. Rehabil.* **84**, 119–124 (2000).

Downloaded from https://www.science.org at The Hong Kong University of Science and Technology (Guangzhou) on May 26, 2026

24. C. H. Ho, R. J. Triolo, A. L. Elias, K. L. Kilgore, A. F. DiMarco, K. Bogie, A. H. Vette, M. L. Audu, R. Kobetic, S. R. Chang, K. M. Chan, S. Dukelow, D. J. Bourbeau, S. W. Brose, K. J. Gustafson, Z. H. T. Kiss, V. K. Mushahwar, Functional electrical stimulation and spinal cord injury. *Phys. Med. Rehabil. Clin. N. Am.* **25**, 631–654 (2014).
25. A. Ramos-Murguialday, D. Broetz, M. Rea, L. Läer, Ö. Yilmaz, F. L. Brasil, G. Liberati, M. R. Curado, E. Garcia-Cossio, A. Vyziotis, W. Cho, M. Agostini, E. Soares, S. R. Soekadar, A. Caria, L. G. Cohen, N. Birbaumer, Brain-machine interface in chronic stroke rehabilitation: A controlled study. *Ann. Neurol.* **74**, 100–108 (2013).
26. A. Caria, C. Weber, D. Brötz, A. Ramos, L. F. Ticini, A. Gharabaghi, C. Braun, N. Birbaumer, Chronic stroke recovery after combined BCI training and physiotherapy: A case report. *Psychophysiology* **48**, 578–582 (2011).
27. S. R. Soekadar, M. Witkowski, J. Mellinger, A. Ramos, N. Birbaumer, L. G. Cohen, ERD-based online brain–machine interfaces (BMI) in the context of neurorehabilitation: Optimizing BMI learning and performance. *IEEE Trans. Nerual Syst. Rehabil. Eng.* **19**, 542–549 (2011).
28. E. R. Buch, A. Modir Shanechi, A. D. Fourkas, C. Weber, N. Birbaumer, L. G. Cohen, Parietofrontal integrity determines neural modulation associated with grasping imagery after stroke. *Brain* **135**, 596–614 (2012).
29. S. Toyama, K. Takano, K. Kansaku, A non-adhesive solid-gel electrode for a non-invasive brain–machine interface. *Front. Neurol.* **3**, 114 (2012).
30. C. Carvalhaes, J. A. de Barros, The surface Laplacian technique in EEG: Theory and methods. *Int. J. Psychophysiol.* **97**, 174–188 (2015).
31. D. J. McFarland, The advantages of the surface Laplacian in brain–computer interface research. *Int. J. Psychophysiol.* **97**, 271–276 (2015).
32. G. Schalk, J. R. Wolpaw, D. J. McFarland, G. Pfurtscheller, EEG-based communication: Presence of an error potential. *Clin. Neurophysiol.* **111**, 2138–2144 (2000).
33. M. Santello, M. Flanders, J. F. Soechting, Postural hand synergies for tool use. *J. Neurosci.* **18**, 10105–10115 (1998).
34. I. M. Bullock, J. Z. Zheng, S. De La Rosa, C. Guertler, A. M. Dollar, Grasp frequency and usage in daily household and machine shop tasks. *IEEE Trans. Haptics* **6**, 296–308 (2013).
35. N. Kapadia, V. Zivanovic, M. Verrier, M. Popovic, Toronto rehabilitation institute–hand function test: Assessment of gross motor function in individuals with spinal cord injury. *Top. Spinal Cord Inj. Rehabil.* **18**, 167–186 (2012).
36. R Core Team, *R: A Language and Environment for Statistical Computing* (R Foundation for Statistical Computing, 2012).
37. J. W. Pratt, Remarks on zeros and ties in the Wilcoxon signed rank procedure. *J. Am. Stat. Assoc.* **54**, 655–667 (1959).
38. J. A. Cohen, Coeffecient of agreement for nominal scales. Educational and psychological measurement. *Educ. Psychol. Meas.* **20**, 37–46 (1960).
39. P. E. Shrout, J. L. Fleiss, Intraclass correlations: Uses in assessing rater reliability. *Psychol. Bull.* **86**, 420–428 (1979).

Acknowledgments: We thank J. Mellinger for help in programming the BNCI platform; the team at Institut Guttmann for support in recruiting the patients, particularly J. E. Prim and M. A. Masbernat; and B. Teufel and M. Nann for assistance in preparing the manuscript. **Funding:** This study was funded by the European Commission under projects AIDE (645322) and WAY (288551), the Deutsche Forschungsgemeinschaft (SO932-2 and Koselleck Project Support), and the German Federal Ministry of Research and Education (BMBF; 01GQ0831 and 16SV5838K). **Author contributions:** S.R.S., M.W., E.O., N.B., and N.V. designed the study. S.R.S., M.W., C.G., M. Cortese, and M. Cempini collected the data. S.R.S., M.W., C.G., M. Cortese, and M. Cempini analyzed the data. S.R.S., M.W., C.G., E.O., M. Cortese, M. Cempini, M.C.C., L.G.C., N.B., and N.V. interpreted the data and performed the literature search. S.R.S., M.W., M. Cortese, M. Cempini, and N.V. wrote the manuscript and created the figures. S.R.S., M.W., C.G., E.O., J.M., M. Cortese, M. Cempini, M.C.C., L.G.C., N.B., and N.V. edited the manuscript. **Competing interests:** N.V., M. Cempini, and M.C.C. are inventors on patent applications (PI2014A000094/EP2890352A2/WO2014033613A2 and US2015223959) submitted by Scuola Superiore Sant'Anna that covers the "wearable exoskeleton device for hand rehabilitation." N.V., M. Cempini, and M.C.C. are co-founders of a spin-off company (IUVO S.r.l.) developing and commercializing exoskeleton technology that may benefit in the future from research presented in this article. Source codes and software used for EEG/EOG B/NHE control is available from the Dryad Digital Repository: http://dx.doi.org/10.5061/dryad.k486f.

Submitted 14 June 2016
Accepted 28 October 2016
Published 6 December 2016
10.1126/scirobotics.aag3296

Citation: S. R. Soekadar, M. Witkowski, C. Gómez, E. Opisso, J. Medina, M. Cortese, M. Cempini, M. C. Carrozza, L. G. Cohen, N. Birbaumer, N. Vitiello, Hybrid EEG/EOG-based brain/neural hand exoskeleton restores fully independent daily living activities after quadriplegia. *Sci. Robot.* **1**, eaag3296 (2016).

Downloaded from https://www.science.org at The Hong Kong University of Science and Technology (Guangzhou) on May 26, 2026

Science Robotics

Hybrid EEG/EOG-based brain/neural hand exoskeleton restores fully independent daily living activities after quadriplegia

S. R. Soekadar, M. Witkowski, C. Gómez, E. Opisso, J. Medina, M. Cortese, M. Cempini, M. C. Carrozza, L. G. Cohen, N. Birbaumer, and N. Vitiello

Sci. Robot. **1** (1), eaag3296. DOI: 10.1126/scirobotics.aag3296

View the article online
https://www.science.org/doi/10.1126/scirobotics.aag3296
Permissions
https://www.science.org/help/reprints-and-permissions

Downloaded from https://www.science.org at The Hong Kong University of Science and Technology (Guangzhou) on May 26, 2026

Use of this article is subject to the Terms of service

Science Robotics (ISSN 2470-9476) is published by the American Association for the Advancement of Science. 1200 New York Avenue NW, Washington, DC 20005. The title *Science Robotics* is a registered trademark of AAAS.

Copyright © 2016, American Association for the Advancement of Science